



Pseudomonas aeruginosa esterase PA2949, a bacterial homolog of the human membrane esterase ABHD6: expression, purification and crystallization

Florian Bleffert,^a Joachim Granzin,^b Holger Gohlke,^{b,c,d} Renu Batra-Safferling,^{b*} Karl-Erich Jaeger^{a,e*} and Filip Kovacic^{a*}

Received 30 October 2018

Accepted 10 February 2019

Edited by A. K. Mitra, University of Auckland, New Zealand

Keywords: *Pseudomonas aeruginosa*; PA2949; esterases; ABHD6; endocannabinoid signalling pathway; Parkinson's disease; Alzheimer's disease.

Supporting information: this article has supporting information at journals.iucr.org/f

^aInstitute of Molecular Enzyme Technology, Heinrich-Heine-Universität Düsseldorf, Forschungszentrum Jülich GmbH, D-52426 Jülich, Germany, ^bInstitute of Complex Systems ICS-6: Structural Biochemistry, Forschungszentrum Jülich GmbH, D-52425 Jülich, Germany, ^cInstitute of Pharmaceutical and Medicinal Chemistry, Heinrich-Heine-Universität Düsseldorf, D-40225 Düsseldorf, Germany, ^dJohn von Neumann Institute for Computing (NIC) and Jülich Supercomputing Centre (JSC), Forschungszentrum Jülich GmbH, D-52425 Jülich, Germany, and ^eInstitute of Bio- and Geosciences IBG-1: Biotechnology, Forschungszentrum Jülich GmbH, D-52426 Jülich, Germany. *Correspondence e-mail: r.batra-safferling@fz-juelich.de, k.-e.jaeger@fz-juelich.de, f.kovacic@fz-juelich.de

The human membrane-bound α/β -hydrolase domain 6 (ABHD6) protein modulates endocannabinoid signaling, which controls appetite, pain and learning, as well as being linked to Alzheimer's and Parkinson's diseases, through the degradation of the key lipid messenger 2-arachidonylglycerol (2-AG). This makes ABHD6 an attractive therapeutic target that lacks structural information. In order to better understand the molecular mechanism of 2-AG-hydrolyzing enzymes, the PA2949 protein from *Pseudomonas aeruginosa*, which has 49% sequence similarity to the ABHD6 protein, was cloned, overexpressed, purified and crystallized. Overexpression of PA2949 in the homologous host yielded the membrane-bound enzyme, which was purified in milligram amounts. Besides their sequence similarity, the enzymes both show specificity for the hydrolysis of 2-AG and esters of medium-length fatty acids. PA2949 in the presence of *n*-octyl β -D-glucoside showed a higher activity and stability at room temperature than those previously reported for PA2949 overexpressed and purified from *Escherichia coli*. A suitable expression host and stabilizing detergent were crucial for obtaining crystals, which belonged to the tetragonal space group $I4_122$ and diffracted to a resolution of 2.54 Å. This study provides hints on the functional similarity of ABHD6-like proteins in prokaryotes and eukaryotes, and might guide the structural study of these difficult-to-crystallize proteins.

1. Introduction

Enzymes of the α/β -hydrolase superfamily are found in virtually all organisms and have functional implications that are important to human health (Lord *et al.*, 2013) and bacterial pathogenesis (Flores-Díaz *et al.*, 2016). The canonical α/β -hydrolase fold consists of up to 11 β -strands folded into a central hydrophobic sheet surrounded by flanking α -helices (Heikinheimo *et al.*, 1999). This fold provides a scaffold for a structurally conserved active site comprising the catalytic triad (Ser, His, Asp) and two oxyanion-hole residues (Heikinheimo *et al.*, 1999). The hydrolytic reactions that are catalyzed by α/β -hydrolases rely on a hydrogen-bond network between the catalytic triad residues that is essential for formation of the nucleophilic serine (Rauwerdink & Kazlauskas, 2015). The residues of the oxyanion hole stabilize the tetrahedral intermediates (Pérez *et al.*, 2012; Rauwerdink & Kazlauskas, 2015).



OPEN ACCESS

Table 1
PA2949 production information.

Source organism	<i>P. aeruginosa</i> PA01
DNA source	<i>P. aeruginosa</i> PA01
Forward primer (5'–3')†	<u>AAACATATGAAACGATTCTC</u>
Reverse primer (5'–3')†	<u>TCAGAGCTCCACCACCACCACCACCAC</u> GCGACCG GCCAC
Cloning vector	pBBR1mcs-3
Expression vector	pBBR- <i>pa2949</i> (Kovacic, Bleffert <i>et al.</i> , 2016)
Cloning host	<i>E. coli</i> DH5 α
Expression host	<i>P. aeruginosa</i> PA01
PA2949-His ₆ amino-acid sequence	MKRFLLGLVLLLAAGAAGVLYFVPATLLASVRTVE RGLAGLSEHSVQVDNLEIAYLEGGSEKNPTLL LIHGFGADKDNWLRFPARPLTERYHVVALDLPG FGDSSKPQQASYDVGTAERVFANFAAAIGVRR LHLAGNSMGHIAALYAARHPEQVLSLALIDN AGVMPARKSELFEFLERGENPLVVRQPEDFQK LLDFVFVQQPPLPAPLKRYPGERAVAASAFNA QIFEQLRQRYIPLEPELPKIEAPTLLWGDRL RVLDVSSIEVMRPLLRKPSVIVIMENCGHVPV ERPEETAQHYQAFLDGVRNAQVAGRRHHHHHE L

† The sequences encoding NdeI and SacI restriction sites are underlined and that encoding the C-terminal His₆ tag is in bold.

Mammals express at least 19 α/β -hydrolases [called α/β -hydrolase domain (ABHD) proteins in the literature], and the biochemical and physiological functions of most of them are largely unknown (Lord *et al.*, 2013). Functional proteomics of brain tissue revealed ABHD6 to be a 2-arachidonylglycerol (2-AG) hydrolase (Blankman *et al.*, 2007). 2-AG is biosynthesized from membrane phospholipid precursors and stimulates cannabinoid (CB) receptors in the vicinity of its own synthesis. A recent study confirmed that ABHD6 controls the levels and signaling efficacy of 2-AG in neurons and is thus considered to be a member of the endocannabinoid signaling pathway (Marrs *et al.*, 2010). This system controls diverse physiological processes such as pain sensation, the maintenance of food intake, learning and memory, and is related to Alzheimer's and Parkinson's diseases (Fernández-Ruiz *et al.*, 2015). Furthermore, ABHD6 is differentially expressed in seven tumor cell lines, with particularly high expression being observed in Ewing family tumors (Lord *et al.*, 2013). Therefore, ABHD6 has been suggested as a new diagnostic marker for these tumors (Max *et al.*, 2009; Lord *et al.*, 2013). Moreover, ABHD6-knockout mice showed reduced body weight, improved glucose homeostasis and insulin action that prevents obesity and type 2 diabetes (Zhao *et al.*, 2016). ABHD6 has emerged as a promising pharmaceutical target, the inhibition of which has been studied biochemically and *in silico* (Feledziak *et al.*, 2012; Bowman & Makriyannis, 2013). However, the three-dimensional structure of ABHD6 remains elusive.

We recently characterized the α/β -hydrolase PA2949 from *P. aeruginosa* (Kovacic, Bleffert *et al.*, 2016). *P. aeruginosa* is a versatile pathogen that causes infections in mammals, plants and insects (Mahajan-Miklos *et al.*, 2000). It mainly infects immunocompromised patients, in particular cystic fibrosis, AIDS and cancer patients (Folkesson *et al.*, 2012). The pathogenicity of *P. aeruginosa* is predominantly related to the production of a large spectrum of cell-associated and cell-secreted virulence factors, among which are several

α/β -hydrolases (Van Delden & Iglewski, 1998; Bofill *et al.*, 2010). PA2949 is a 34.8 kDa protein that shows esterase activity and is anchored to the *E. coli* membrane by a putative N-terminal transmembrane domain (Kovacic, Bleffert *et al.*, 2016). PA2949 contains a typical α/β -hydrolase Ser–His–Asp catalytic triad, as shown previously in our mutagenesis studies (Kovacic, Bleffert *et al.*, 2016).

Here, we report the expression in the homologous host *P. aeruginosa*, purification from membranes, crystallization and preliminary X-ray analysis of PA2949, a bacterial homolog of human ABHD6. To date, no structure is available of a protein containing an ABHD6-like domain. Therefore, the structure of the putatively single-pass integral membrane protein PA2949 should contribute to the understanding of the function of these proteins, with potential therapeutic implications.

2. Materials and methods

2.1. Overexpression and purification

P. aeruginosa PA01 cells harboring pBBR-*pa2949* (Kovacic, Bleffert *et al.*, 2016) were cultivated overnight in Luria–Bertani (LB) medium supplemented with tetracycline (100 $\mu\text{g ml}^{-1}$) at 37°C (Table 1). This culture was used to inoculate an expression culture in LB medium supplemented with tetracycline (100 $\mu\text{g ml}^{-1}$) to an initial OD_{580 nm} of 0.05. The cultures were grown at 37°C until they reached an OD_{580 nm} of ~ 1 . The cells were harvested by centrifugation (15 min at 6750g and 4°C), resuspended in 100 mM Tris–HCl buffer pH 8 and disrupted using a French press. PA2949 was purified from the membrane fraction by immobilized metal-affinity chromatography (IMAC) using Ni–NTA agarose (Qiagen, Hilden, Germany) as described previously (Kovacic, Bleffert *et al.*, 2016), with the modification that the Triton X-100 in the elution buffer was replaced by 30 mM *n*-octyl β -D-glucoside (OG). The PA2949 samples eluted from the Ni–NTA column were transferred into 100 mM Tris–HCl buffer pH 8 supplemented with 30 mM *n*-octyl β -D-glucoside (OG) by gel filtration using a PD-10 column (GE Healthcare, Solingen, Germany) according to the manufacturer's protocol. This PA2949 sample was loaded onto an anion-exchange chromatography column containing UNOsphere Q medium (Bio-Rad Laboratories, Munich, Germany) equilibrated with 100 mM Tris–HCl pH 8 buffer containing 30 mM OG. Purified PA2949 was collected in the flowthrough fraction and the protein impurities were retained on the column. The purified PA2949 was stored at room temperature.

2.2. SDS–PAGE, preparation of antisera and immunodetection

Proteins were analyzed by sodium dodecyl sulfate–polyacrylamide gel electrophoresis (SDS–PAGE) under denaturing conditions on 12% (w/v) gels as described by Laemmli (1970). SDS–PAGE slices containing PA2949 were used to raise polyclonal antisera in rabbits (Eurogentec, Seraing, Belgium) by injecting 100 μg antigen four times over

three months. The proteins transferred from the SDS–PAGE gel to PVDF membranes by Western blotting (Yuen *et al.*, 1989) were detected using anti-PA2949 specific antiserum according to the following procedure. The PVDF membrane with transferred proteins was saturated for 1 h in 25 mM Tris–HCl buffer pH 8 containing 150 mM NaCl, 3 mM KCl, 0.2% (v/v) Tween-20 and 5% (w/v) skimmed milk, followed by incubation with anti-PA2949 antiserum diluted 5000 times with the same buffer as used for saturation. The membrane was washed three times with 25 mM Tris–HCl buffer pH 8 containing 150 mM NaCl, 3 mM KCl and 0.2% (v/v) Tween-20, incubated for 1 h with goat anti-rabbit immunoglobulin G antibodies coupled to HRP (horseradish peroxidase; Sigma, St Louis, USA) according to the manufacturer's instructions, washed again three times with 25 mM Tris–HCl buffer pH 8 containing 150 mM NaCl, 3 mM KCl and 0.2% (v/v) Tween-20, and then exposed with an ECL Western blotting detection kit (Amersham Bioscience, Freiburg). The protein concentration was determined by measuring the $A_{280\text{ nm}}$ using a NanoDrop 2000c spectrophotometer (ThermoFisher Scientific Inc., Waltham, Massachusetts, USA) and using an extinction coefficient ($\epsilon = 22\,920\text{ M}^{-1}\text{ cm}^{-1}$) for PA2949 with a His₆ tag calculated using the *ProtParam* tool (Navia-Paldanius *et al.*, 2012).

2.3. Enzyme-activity assays

Enzyme activities towards fatty-acid esters of *p*-nitrophenol (*p*-NP) were determined according to a previously described method (Kovacic, Bleffert *et al.*, 2016). The enzymatic reactions were performed in a 96-well microplate by adding 5 μl (8 nM) of enzyme sample to 150 μl of the substrate. The kinetic parameters K_m and k_{cat} were determined by measuring the PA2949 activity with 0.05, 0.1, 0.2, 0.3, 0.5 and 1 mM *p*-nitrophenyl butyrate; the data were fitted to the Michaelis–Menten equation using a nonlinear regression method.

Triacylglyceride (Sigma, Taufkirchen, Germany) and 2-AG (Avanti, Alabaster, USA) substrates were prepared for enzyme-activity assays (25 μl enzyme + 25 μl substrate) as described previously (Jaeger & Kovacic, 2014). The amount of fatty acids released by PA2949 was determined using a NEFA-HR(2) kit (Wako Chemicals, Neuss, Germany).

2.4. Thermal stability

Fluorescence-based thermal stability experiments were performed using a Prometheus NT.48 from NanoTemper Technologies. Capillaries containing 10 μl PA2949 sample were inserted into the machine, the temperature was increased from 20 to 90°C at a rate of 1°C min⁻¹, and the fluorescence was measured at emission wavelengths of 330 and 350 nm. Enzyme activity-based thermal unfolding experiments were performed by measuring the residual esterase activity of a PA2949 sample incubated for 1 h at temperatures from 30 to 70°C. The enzyme assay was performed as described above using *p*-NPC₄ substrate. The ratio of fluorescence intensities at 350 and 330 nm (for the biophysical method) and esterase activities (for the biochemical method) as a function of

Table 2
Crystallization conditions.

Method	Sitting-drop vapor diffusion
Plate type	NeXtal Evolution μ plate (Qiagen, Hilden, Germany)
Temperature (°C)	19
Protein concentration (mg ml ⁻¹)	3.5
Buffer composition of protein solution	100 mM Tris–HCl pH 8, 30 mM OG
Composition of reservoir solution	100 mM trisodium citrate pH 5.6 with 10% (w/v) PEG 4000 and 10% (w/v) propan-2-ol
Volume, ratio of drop	2 μl , 1:1
Volume of reservoir (μl)	70

temperature were used to determine the transition temperatures, which can be interpreted as the melting temperatures.

2.5. Crystallization and data collection

For crystallization, purified PA2949 was concentrated to 3.5 mg ml⁻¹ using an ultrafiltration device with a 30 kDa molecular-weight cutoff membrane. Initial crystallization screening was performed with the AmSO₄, CubicPhase I and CubicPhase II, MbClass, PEGs I and PEGs II Suites (Qiagen, Hilden, Germany), Crystal Screen and Crystal Screen 2 (Hampton Research, Aliso Viejo, California, USA) and Wizard Screens 1 and 2 (Emerald BioStructures, Bainbridge Island, Washington, USA) crystallization screening kits at 19°C using the sitting-drop vapor-diffusion method (Table 2). The PA2949 crystals used for X-ray diffraction were grown from a solution consisting of 1 μl PA2949 solution and 1 μl reservoir solution [100 mM trisodium citrate pH 5.6 with 10% (w/v) PEG 4000 and 10% (w/v) propan-2-ol]. Crystals appeared within three weeks. Before cryocooling, single crystals were soaked stepwise in reservoir solution containing up to 15% (w/v) polyethylene glycol 200. The X-ray diffraction data were recorded on beamline ID23-1 at the European Synchrotron Radiation Facility, Grenoble, France using a wavelength of 0.9791 Å. The data-collection strategies, taking radiation damage into account, were based on calculations using *BEST* (Bourenkov & Popov, 2010). Data processing was carried out using *XDS* (Kabsch, 2010) and *AIMLESS* (which is part of the *CCP4* software package; Winn *et al.*, 2011). Structure determination is currently being performed by molecular replacement.

3. Results and discussion

3.1. Similarity of *P. aeruginosa* PA2949 and human ABHD6

Previously, we have described *P. aeruginosa* PA2949 as a membrane-bound esterase that is homologous to bacterial esterases/lipases (Kovacic, Bleffert *et al.*, 2016). PA2949 shows 27% sequence identity and 49% sequence similarity to the human α/β -hydrolase domain 6 (ABHD6) protein, which exerts lipase activity (Blankman *et al.*, 2007; Fig. 1a). Secondary-structure prediction revealed a similar organization of eight β -strands and ten α -helices in both proteins (Fig. 1b). Sequence analysis revealed conservation of Ser137 in PA2949

and Ser148 in ABHD6, which yielded inactive enzymes when mutated to alanine (Kovacic, Bleffert *et al.*, 2016; Navia-Paldanius *et al.*, 2012). Inhibition experiments with PA2949 and ABHD6 revealed similar inhibition profiles with respect to the typical lipase inhibitor tetrahydrolipstatin (THL; Ašler *et al.*, 2007) and the arylesterase inhibitor phenylmethylsulfonyl fluoride (PMSF; Blankman *et al.*, 2007; Kovacic, Bleffert *et al.*, 2016). Furthermore, the other two putative members of the catalytic triad (His and Asp) and the putative oxyanion-hole residues (Met and Phe) are strictly conserved between the two enzymes (Fig. 1). The putative acyltransferase motif (HXXXXD, where *X* represents any residue) reported for ABHD6 (Lord *et al.*, 2013) is also conserved in PA2949 (Fig. 1*a*). Although promiscuous enzymes with lipase and acyltransferase activities have previously been described (Brumlik & Buckley, 1996; Vijayaraj *et al.*, 2012), the acyltransferase activity of ABHD6 and PA2949 still needs to be demonstrated experimentally. Prediction of cellular localization revealed a putative N-terminal transmembrane (TM) domain (Fig. 1), which is likely to serve as a signal anchor, in both proteins (Kovacic, Bleffert *et al.*, 2016; Lord *et al.*, 2013). This suggestion is supported by the experimentally demonstrated membrane localization of PA2949 and ABHD6 (Blankman *et al.*, 2007; Kovacic, Bleffert *et al.*, 2016). To conclude, comparison of the sequence properties of PA2949 and ABHD6 revealed substantial similarity despite the considerable evolutionary distance between them.

3.2. Optimized expression and purification procedure for *P. aeruginosa* PA2949

For the crystallographic characterization of PA2949, we attempted to purify milligram amounts of PA2949 under

conditions where it retains activity during the time frame of the crystallization experiments. Our previously published system for the expression of PA2949 in *E. coli* BL21(DE3) cells (Kovacic, Bleffert *et al.*, 2016) and purification by immobilized metal-affinity chromatography in the presence of Triton X-100 yielded a protein that showed a loss of enzymatic activity after storage at 4 or -20°C in the presence or absence of glycerol (data not shown). To overcome the protein stability issue, we tested whether the homologous host *P. aeruginosa* might be more suitable for the expression of membrane-bound PA2949 than a heterologous host. We developed the *P. aeruginosa* PA01 system for induction-independent constitutive expression of PA2949 controlled by a moderate *lac* promoter on the pBBR1mcs-3 plasmid. *P. aeruginosa* PA01 cells carrying the pBBR-*pa2949* plasmid (Kovacic, Bleffert *et al.*, 2016) expressed catalytically active PA2949 in the late logarithmic and stationary phases. While the esterase activity was constant during growth, degradation of intracellular PA2949 in the stationary-phase culture was observed as judged from Western blot analysis (Fig. 2). Consequently, for purification purposes cells were harvested in the late logarithmic phase (an $\text{OD}_{580\text{ nm}}$ of ~ 1) to avoid the degradation of PA2949 observed in cultures with an $\text{OD}_{580\text{ nm}}$ of 2 (Fig. 2).

The selection of a detergent to provide stable conditions for membrane proteins after their extraction from bacterial membranes is essential for subsequent characterization. The mild, non-ionic detergent Triton X-100, widely used for solubilizing proteins from membranes (Schnaitman, 1971; Slinde & Flatmark, 1976), showed a good performance in solubilizing *P. aeruginosa* membranes (Kovacic, Bleffert *et al.*, 2016). However, denaturation of a membrane protein can be caused by Triton X-100 owing to suboptimal stabilization of the TM domains (Seddon *et al.*, 2004; Garavito & Ferguson-Miller,

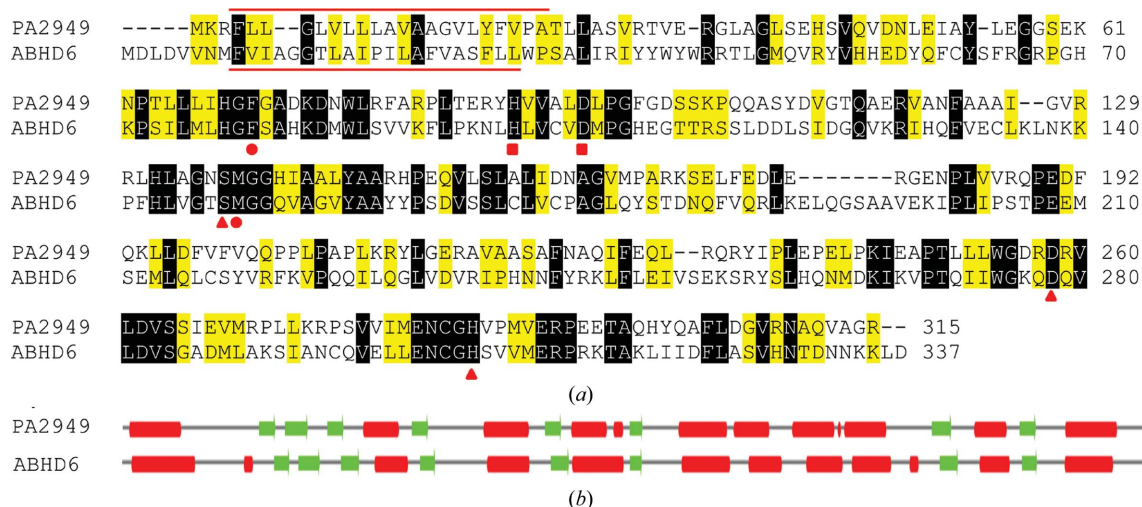


Figure 1

Sequence alignment of *P. aeruginosa* PA2949 with human ABHD6 and secondary-structure prediction. (a) Sequence alignment. The putative active site comprising the catalytic triad (Ser148, His306 and Asp278 in ABHD6, and Ser137, His286 and Asp258 in PA2949) and the oxyanion-hole residues (Phe80 and Met149 in ABHD6, and Phe71 and Met138 in PA2949) are indicated by red triangles and circles, respectively. Conserved residues (His99 and Asp104 in ABHD6 and His90 and Asp95 in PA2949) of the putative HXXXXD acyltransferase motif are indicated by red squares. The putative transmembrane domains of PA2949 (amino acids 4–24) and ABHD6 (amino acids 9–29) are indicated by red lines above and below the sequences, respectively. Identical and similar residues are shaded in black and yellow, respectively. The pairwise sequence alignment was generated with the *EMBOSS Water* (Rice *et al.*, 2000) local alignment tool from the European Bioinformatics Institute (EMBL–EBI). (b) Secondary structure was predicted with the *JPred4* server (Drozdetskiy *et al.*, 2015) using a method based on hidden Markov models. α -Helices are indicated in red and β -sheets in green.

2001), destabilization of extramembranous soluble domains (Yang *et al.*, 2014) or by reactive peroxides that are products of the oxidation and hydrolysis of Triton X-100 (Ashani & Catravas, 1980; Moraes *et al.*, 2014). For these reasons, we applied the mild, non-ionic detergent OG, commonly used in membrane-protein research (Moraes *et al.*, 2014; Arolas *et al.*, 2014), to PA2949. The PA2949 sample eluted from the IMAC column using a buffer that contains OG showed the presence of other protein impurities (Fig. 3), as also observed for purification from *E. coli* (Kovacic, Bleffert *et al.*, 2016). We next purified PA2949 by anion-exchange chromatography to a homogeneity that was sufficient for further biochemical and crystallographic studies (Fig. 3). The OG-stabilized PA2949 protein retained more than 56% of its esterase activity, as measured with *p*-nitrophenyl (*p*-NP) hexanoate (C₆) substrate, after storage at room temperature for six months. The thermal stability of PA2949 in OG was studied by measuring the change in intrinsic protein fluorescence upon thermal unfolding and by measuring the residual esterase activity after the exposure of PA2949 to different temperatures. These experiments revealed melting temperatures of PA2949 of 43.4 ± 0.5 and 53.1 ± 0.4°C calculated from enzyme-activity and fluorescence measurements, respectively (Fig. 4). It is likely that differences in the experimental setup (1 h of incubation in the enzymatic method *versus* continuous heating in the nanoDSF method) led to the observed discrepancy in the melting temperatures.

3.3. Substrate specificity of *P. aeruginosa* PA2949

PA2949 purified from *P. aeruginosa* in the presence of OG showed a 2.3-fold higher esterase activity than the enzyme purified from *E. coli* with Triton X-100 (198.8 ± 5.1 U mg⁻¹; Kovacic, Bleffert *et al.*, 2016) using *p*-NPC₆ as a substrate (Table 3). Substrate-specificity measurements revealed the highest activity of PA2949 to be with *p*-NP octanoate (C₈), and that the activity declines with increasing length of the fatty-

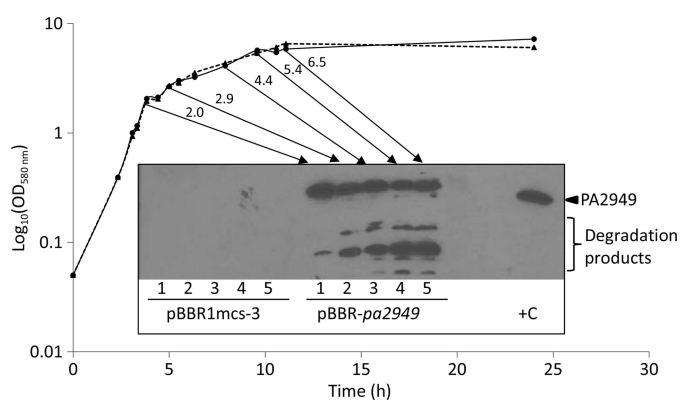


Figure 2 Expression of PA2949 in *P. aeruginosa*. *P. aeruginosa* PA01 strain carrying pBBR1mcs-3 (empty-vector control, dashed line) or pBBR-*pa2949* (solid line) was grown in LB medium at 37°C; cells were collected at five (1–5) different growth stages (the respective OD_{580 nm} values are indicated above the arrows). Cells equivalent to 100 µl of culture with an OD_{580 nm} of 1 were analyzed by SDS–PAGE and the presence of PA2949 in each sample was tested by Western blotting using anti-His-tag antibodies. Purified PA2949 (+C) was used as a positive control.

Table 3

Substrate specificities of PA2949 with *p*-nitrophenyl (*p*-NP) esters and triacylglycerides (TAG).

Acyl-chain length	<i>p</i> -NP activity† (U mg ⁻¹)	TAG activity† (mU mg ⁻¹)
C ₂	108.9 ± 6.5	NA
C ₄	520.4 ± 31.7	NA
C ₆	458.0 ± 11.5	10.1 ± 0.2
C ₈	621.2 ± 34.2	ND
C ₁₀	351.3 ± 25.5	12.6 ± 0.2
C ₁₂	162.5 ± 12.5	3.9 ± 0.2
C ₁₄	58.9 ± 19.4	0.3 ± 0.1
C ₁₆	18.4 ± 5.1	NA
C ₁₈	NA	NA

† All values are the mean ± standard deviation of three independent measurements of each set in triplicate. NA, not active; ND, not determined.

acid acyl chain to reach no measurable activity with *p*-NP stearate (C₁₈) (Table 3). PA2949 hydrolyses natural triacylglycerol substrates with a similar specificity as *p*-NP esters, although its activity with triglycerides was lower (Table 3). Apparently, PA2949 shows a typical activity profile for esterases that are capable of releasing medium-chain fatty acids from water-soluble carboxylic esters (Leščič Ašler *et al.*, 2010; Kovacic, Mandrysch *et al.*, 2016; Chow *et al.*, 2012; Ali *et al.*, 2012). Kinetics measurements of the hydrolysis of a typical esterase substrate, *p*-NP butyrate (C₄), revealed that PA2949 follows Michaelis–Menten kinetics, as reported for most esterases (Fig. 5). Interestingly, ABHD6 also hydrolyses TAG substrates and shows a preference for esters with medium-chain acyl chains (from C₈ to C₁₄; Navia-Paldanius *et al.*, 2012).

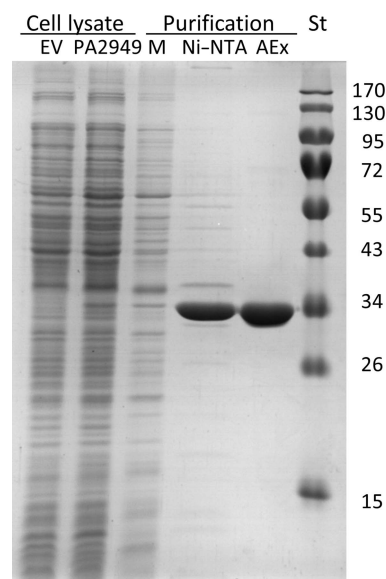
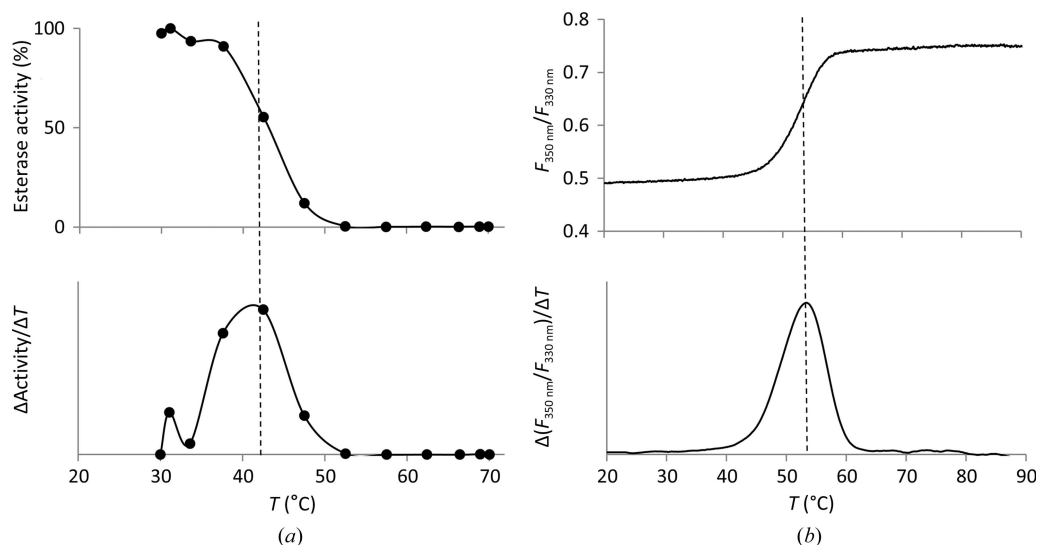
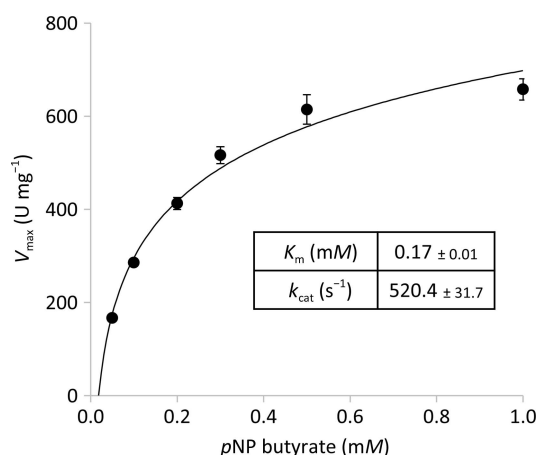


Figure 3 Purification of PA2949 from *P. aeruginosa*. (a) *P. aeruginosa* PA01 cells carrying the *pa2949* expression vector (pBBR-*pa2949*) or pBBR1mcs-3 (EV, empty vector) were harvested at an OD_{580 nm} of 1 and disrupted. Membranes (M) were separated by ultracentrifugation. PA2949 was purified with a Ni–NTA column and subsequently with a UNOsphere Q anion-exchange column (AEx) in the presence of *n*-octyl β-D-glucoside. The samples were analyzed by SDS–PAGE stained with Coomassie Brilliant Blue G-250. The molecular weights of protein standards (St) are indicated on the right in kDa.


Figure 4

Thermal stability of PA2949 in OG buffer measured by determination of enzymatic activity (a) and change in intrinsic fluorescence (b). The relative esterase activity and the derivative of esterase activity ($\Delta\text{Activity}/\Delta T$) as a function of temperature are shown in the upper and lower panels, respectively. 100% activity corresponds to the highest measured activity of PA2949. The fluorescence ratio ($F_{350\text{ nm}}/F_{330\text{ nm}}$) and the derivative of the fluorescence ratio $[\Delta(F_{350\text{ nm}}/F_{330\text{ nm}})]/\Delta T$ as a function of temperature are shown in the upper and lower diagrams, respectively. Dashed lines indicate calculated melting temperatures. Enzyme-activity results represent measurements of three independent experiments each with at least three samples. Standard deviations were within 10%. The fluorescence-based unfolding result is a representative single curve.

However, *in vitro* measurements showed a high activity of ABHD6 against the natural substrate 2-AG, which contains a long-chain fatty acid of 20 C atoms and four unsaturated bonds (Navia-Paldanius *et al.*, 2012). Our results with purified PA2949 demonstrated that the enzyme rapidly releases the fatty acid from the 2-AG substrate with an activity of 12.2 ± 0.3 nanomoles of fatty acid per milligram of PA2949 per minute. This activity is in the region of the activity reported for ABHD6 (7.4 ± 0.5 nanomoles of fatty acid per milligram of ABHD6 per minute), although these measurements were performed with lysates of human cells transiently expressing ABHD6 (Navia-Paldanius *et al.*, 2012). To conclude, the substrate profiling of PA2949 suggests that PA2949 and


Figure 5

Enzyme kinetics of PA2949. The esterase activity of PA2949 (8 nM) purified with OG was measured using pNP C₄, and kinetic parameters (\pm standard deviation) were determined by nonlinear regression analysis of data fitted to the Michaelis–Menten equation. The results represent measurements from eight independent experiments.

Table 4

X-ray diffraction data-collection and processing statistics for PA2949.

Values in parentheses are for the highest resolution shell.

Beamline	ID23-1
Detector	PILATUS 6M
Wavelength (Å)	0.9791
Resolution range (Å)	47.86–2.54 (2.65–2.54)
Space group	<i>I</i> 4 ₁ 22
<i>a</i> , <i>b</i> , <i>c</i> (Å)	135.36, 135.36, 205.29
α , β , γ (°)	90, 90, 90
Total reflections	179853
Unique reflections	31637 (3807)
Multiplicity	5.7 (5.9)
Completeness (%)	99.7 (99.9)
Mean <i>I</i> / σ (<i>I</i>)	8.8 (1.3)
Wilson <i>B</i> factor (Å ²)	45.91
<i>R</i> _{merge}	0.148 (1.656)
<i>R</i> _{meas}	0.162 (1.813)
<i>R</i> _{p.i.m.}	0.067 (0.730)
Mn(<i>I</i>) half-set correlation CC _{1/2}	0.994 (0.419)
Expected No. of molecules in asymmetric unit	2
Solvent fraction (%)	58
Matthews coefficient (Å ³ Da ⁻¹)	2.9

ABHD6 are biochemically similar, which is in agreement with the sequence similarity and the similarities in their inhibition results and cellular localization. Although the role of arachidonic acid as a precursor of signaling messengers in eukaryotes has been established, limited data are available on its presence and function in prokaryotes (Bajpai & Bajpai, 1992; Martínez & Campos-Gómez, 2016). The physiological relevance of the 2-AG hydrolase activity of PA2949 still needs to be elucidated.

3.4. Crystallization of PA2949

Proteins with a single TM domain are considered to be difficult to crystallize, which is the reason why few structures

of them are available (Monk *et al.*, 2014; Ray *et al.*, 2018). The concentrated PA2949 sample (3.5 mg ml^{-1}) was centrifuged ($21\,000g$, 10 min) prior to performing crystallization setups. Single crystals were obtained using the sitting-drop vapor-diffusion method at 19°C after a few rounds of fine screening around the buffer conditions described in Section 2. Tetragonal crystals of approximate dimensions $180 \times 40 \times 40 \mu\text{m}$ grew after an equilibration period of three weeks (Fig. 6). These crystals diffracted to 2.54 \AA resolution. Data processing revealed the space group to be $I4_122$, with unit-cell parameters $a = b = 135.36$, $c = 205.29 \text{ \AA}$, $\alpha = \beta = \gamma = 90^\circ$. A summary of the X-ray crystallographic data-collection statistics is presented in Table 4. The calculated Matthews coefficient and the solvent

content were $2.9 \text{ \AA}^3 \text{ Da}^{-1}$ and 58%, respectively. This suggests the presence of two molecules in the asymmetric unit of the PA2949 crystals. Currently, we are fine-tuning the crystallization conditions to improve the quality of the crystals for successful structure determination using the molecular-replacement method. The high-resolution crystal structure of PA2949 will provide information on the α/β -hydrolase class of proteins, which could be important in order to understand their structure–function relationship.

Acknowledgements

We are grateful to the beamline scientists at the European Synchrotron Radiation Facility, Grenoble, France for assisting with the use of beamline ID23-1. We acknowledge Vinko Misetic and Moran Jerabek from NanoTemper Technologies GmbH, Munich, Germany for providing the device for thermal stability measurements.

Funding information

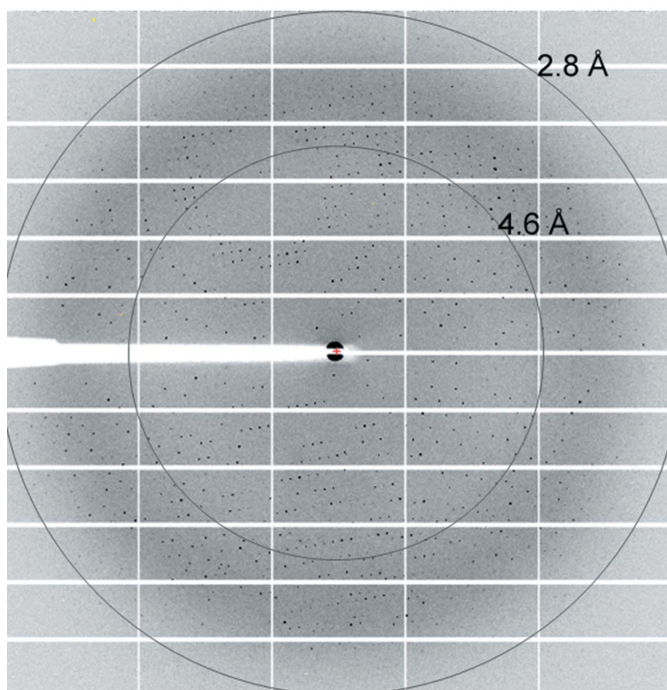
This study was supported by Deutsche Forschungsgemeinschaft grant CRC1208 (projects A02 and A03).

References

- Ali, Y. B., Verger, R. & Abousalham, A. (2012). *Methods Mol. Biol.* **861**, 31–51.
- Arolas, J. L., García-Castellanos, R., Goulas, T., Akiyama, Y. & Gomis-Rüth, F. X. (2014). *Protein Expr. Purif.* **99**, 113–118.
- Ashani, Y. & Catravas, G. N. (1980). *Anal. Biochem.* **109**, 55–62.
- Ašler, I. L., Zehl, M., Kovačić, F., Müller, R., Abramić, M., Allmaier, G. & Kojić-Prodić, B. (2007). *Biochim. Biophys. Acta*, **1770**, 163–170.
- Bajpai, P. & Bajpai, P. K. (1992). *Biotechnol. Appl. Biochem.* **15**, 1–10.
- Blankman, J. L., Simon, G. M. & Cravatt, B. F. (2007). *Chem. Biol.* **14**, 1347–1356.
- Bofill, C., Prim, N., Mormeneo, M., Manresa, A., Javier Pastor, F. I. & Diaz, P. (2010). *Biochimie*, **92**, 307–316.
- Bourenkov, G. P. & Popov, A. N. (2010). *Acta Cryst. D* **66**, 409–419.
- Bowman, A. L. & Makriyannis, A. (2013). *Chem. Biol. Drug Des.* **81**, 382–388.
- Brumlik, M. J. & Buckley, J. T. (1996). *J. Bacteriol.* **178**, 2060–2064.
- Chow, J., Kovacic, F., Dall Antonia, Y., Krauss, U., Fersini, F., Schmeisser, C., Lauinger, B., Bongen, P., Pietruszka, J., Schmidt, M., Menyes, I., Bornscheuer, U. T., Eckstein, M., Thum, O., Liese, A., Mueller-Diekmann, J., Jaeger, K. E. & Streit, W. R. (2012). *PLoS One*, **7**, e47665.
- Drozdzetskiy, A., Cole, C., Procter, J. & Barton, G. J. (2015). *Nucleic Acids Res.* **43**, W389–W394.
- Feledziak, M., Lambert, D. M., Marchand-Brynaert, J. & Muccioli, G. G. (2012). *Recent Pat. CNS Drug. Discov.* **7**, 49–70.
- Fernández-Ruiz, J., Romero, J. & Ramos, J. A. (2015). *Handb. Exp. Pharmacol.* **231**, 233–259.
- Flores-Díaz, M., Monturiol-Gross, L., Naylor, C., Alape-Girón, A. & Flieger, A. (2016). *Microbiol. Mol. Biol. Rev.* **80**, 597–628.
- Folkesson, A., Jelsbak, L., Yang, L., Johansen, H. K., Ciofu, O., Høiby, N. & Molin, S. (2012). *Nat. Rev. Microbiol.* **10**, 841–851.
- Garavito, R. M. & Ferguson-Miller, S. (2001). *J. Biol. Chem.* **276**, 32403–32406.
- Heikinheimo, P., Goldman, A., Jeffries, C. & Ollis, D. L. (1999). *Structure*, **7**, R141–R146.
- Jaeger, K. E. & Kovacic, F. (2014). *Methods Mol. Biol.* **1149**, 111–134.
- Kabsch, W. (2010). *Acta Cryst. D* **66**, 125–132.



(a)



(b)

Figure 6

Crystal and initial X-ray diffraction pattern of PA2949. (a) A tetragonal PA2949 crystal in a loop prepared for collection of the diffraction pattern. (b) X-ray diffraction pattern from a reference set of two images taken with a resolution of $\sim 2.8 \text{ \AA}$ (edge of the detector) with a maximum φ separation of 90° with $\Delta\varphi = 1^\circ$. The optimal strategy for data collection was determined based on these images using *MOSFLM* (Winn *et al.*, 2011) and *BEST* (Bourenkov & Popov, 2010). The given resolution for data collection was 2.5 \AA (for results, see Table 4).

- Kovacic, F., Bleffert, F., Caliskan, M., Wilhelm, S., Granzin, J., Batra-Safferling, R. & Jaeger, K. E. (2016). *FEBS Open Bio*, **6**, 484–493.
- Kovacic, F., Mandrysch, A., Poojari, C., Strodel, B. & Jaeger, K. E. (2016). *Protein Eng. Des. Sel.* **29**, 65–76.
- Laemmli, U. K. (1970). *Nature (London)*, **227**, 680–685.
- Lešćić Ašler, I., Ivić, N., Kovačić, F., Schell, S., Knorr, J., Krauss, U., Wilhelm, S., Kojić-Prodić, B. & Jaeger, K.-E. (2010). *ChemBioChem*, **11**, 2158–2167.
- Lord, C. C., Thomas, G. & Brown, J. M. (2013). *Biochim. Biophys. Acta*, **1831**, 792–802.
- Mahajan-Miklos, S., Rahme, L. G. & Ausubel, F. M. (2000). *Mol. Microbiol.* **37**, 981–988.
- Marrs, W. R., Blankman, J. L., Horne, E. A., Thomazeau, A., Lin, Y. H., Coy, J., Bodor, A. L., Muccioli, G. G., Hu, S. S.-J., Woodruff, G., Fung, S., Lafourcade, M., Alexander, J. P., Long, J. Z., Li, W., Xu, C., Möller, T., Mackie, K., Manzoni, O. J., Cravatt, B. F. & Stella, N. (2010). *Nat. Neurosci.* **13**, 951–957.
- Martínez, E. & Campos-Gómez, J. (2016). *Nat. Commun.* **7**, 13823.
- Max, D., Hesse, M., Volkmer, I. & Staeger, M. S. (2009). *Cancer Sci.* **100**, 2383–2389.
- Monk, B. C., Tomasiak, T. M., Keniya, M. V., Huschmann, F. U., Tyndall, J. D., O'Connell, J. D., Cannon, R. D., McDonald, J. G., Rodriguez, A., Finer-Moore, J. S. & Stroud, R. M. (2014). *Proc. Natl Acad. Sci. USA*, **111**, 3865–3870.
- Moraes, I., Evans, G., Sanchez-Weatherby, J., Newstead, S. & Shaw Stewart, P. D. (2014). *Biochim. Biophys. Acta*, **1838**, 78–87.
- Navia-Paldanius, D., Savinainen, J. R. & Laitinen, J. T. (2012). *J. Lipid Res.* **53**, 2413–2424.
- Pérez, D., Kovacic, F., Wilhelm, S., Jaeger, K. E., García, M. T., Ventosa, A. & Mellado, E. (2012). *Microbiology*, **158**, 2192–2203.
- Rauwerdink, A. & Kazlauskas, R. J. (2015). *ACS Catal.* **5**, 6153–6176.
- Ray, L. C., Das, D., Entova, S., Lukose, V., Lynch, A. J., Imperiali, B. & Allen, K. N. (2018). *Nat. Chem. Biol.* **14**, 538–541.
- Rice, P., Longden, I. & Bleasby, A. (2000). *Trends Genet.* **16**, 276–277.
- Schnaitman, C. A. (1971). *J. Bacteriol.* **108**, 545–552.
- Seddon, A. M., Curnow, P. & Booth, P. J. (2004). *Biochim. Biophys. Acta*, **1666**, 105–117.
- Slinde, E. & Flatmark, T. (1976). *Biochim. Biophys. Acta*, **455**, 796–805.
- Van Delden, C. & Iglewski, B. H. (1998). *Emerg. Infect. Dis.* **4**, 551–560.
- Vijayaraj, P., Jashal, C. B., Vijayakumar, A., Rani, S. H., Venkata Rao, D. K. & Rajasekharan, R. (2012). *Plant Physiol.* **160**, 667–683.
- Winn, M. D., Ballard, C. C., Cowtan, K. D., Dodson, E. J., Emsley, P., Evans, P. R., Keegan, R. M., Krissinel, E. B., Leslie, A. G. W., McCoy, A., McNicholas, S. J., Murshudov, G. N., Pannu, N. S., Potterton, E. A., Powell, H. R., Read, R. J., Vagin, A. & Wilson, K. S. (2011). *Acta Cryst. D* **67**, 235–242.
- Yang, Z., Wang, C., Zhou, Q., An, J., Hildebrandt, E., Aleksandrov, L. A., Kappes, J. C., DeLucas, L. J., Riordan, J. R., Urbatsch, I. L., Hunt, J. F. & Brouillette, C. G. (2014). *Protein Sci.* **23**, 769–789.
- Yuen, S. W., Chui, A. H., Wilson, K. J. & Yuan, P. M. (1989). *Biotechniques*, **7**, 74–83.
- Zhao, S., Mugabo, Y., Ballentine, G., Attane, C., Iglesias, J., Poursharifi, P., Zhang, D., Nguyen, T. A., Erb, H., Prentki, R., Peyot, M.-L., Joly, E., Tobin, S., Fulton, S., Brown, J. M., Madiraju, S. R. M. & Prentki, M. (2016). *Cell Rep.* **14**, 2872–2888.